JOURNAL OF VIROLOGY, May 2000, p. 4273–4283 Vol. 74, No. 9
0022-538X/00/$04.00+0

Rescue of Multiple Viral Functions by a Second-Site Suppressor of a Human Immunodeficiency Virus Type 1 Nucleocapsid Mutation

ANDREA CIMARELLI,[1] SARA SANDIN,[2] STEFAN HÖGLUND,[2] AND JEREMY LUBAN[1,3]*

Departments of Microbiology[1] and Medicine,[3] Columbia University College of Physicians and Surgeons, New York, New York 10032, and Department of Biochemistry, Biomedical Center, Uppsala, Sweden[2]

Received 30 November 1999/Accepted 25 January 2000

Human immunodeficiency type 1 (HIV-1) bearing the nucleocapsid (NC) mutation R10A/K11A is replication defective. After serial passage of the mutant virus in tissue culture, we isolated a revertant that retained the original mutation. It had acquired, in addition, a new mutation (E21K) that was formally demonstrated to be sufficient for restoration of viral replication. Detailed analysis of the replication defect of R10A/K11A revealed a threefold reduction in virion yield and a fivefold reduction in packaging of viral genomic RNA. Real-time PCR was then used to quantitate viral DNA synthesis following infection of Jurkat T cells. After adjustment for the assembly and packaging defects, a minor (twofold) reduction in synthesis of either strong-stop, full-length linear DNA or 2-LTR circles was observed with R10A/K11A virions, indicating that reverse transcription and nuclear transport of the viral genome were largely intact. However, after adjustment for the amounts of full-length or 2-LTR circles produced, R10A/K11A virions were at least 10-fold less infectious than wild type, indicating that viral DNA produced by the R10A/K11A mutant failed to integrate. Each of the above-mentioned defects was corrected by introduction of the second-site compensatory mutation E21K. These results demonstrate that the replication defect of mutant R10A/K11A can be explained by impairment at multiple steps in the viral life cycle, most important among them being integration and RNA packaging. The E21K mutation is predicted to restore positive charge to the face of the R10A/K11A mutant NC protein that interacts with the HIV-1 SL3 RNA stem-loop, emphasizing the importance of NC basic residues for HIV-1 replication.

Retroviral nucleocapsid (NC) proteins are expressed as part of a Gag polyprotein precursor which is cleaved by the virus-encoded protease during virion maturation (reviewed in references 29 and 47). With the exception of spumaviruses, NC proteins encoded by different retroviruses share two structural characteristics: the presence of either one or two Cys-His box motifs (Cys-X_2-Cys-X_4-His-X_4-Cys) and a large number of basic residues distributed throughout the protein (reviewed in references 5 and 63).

NC plays roles in nearly all steps of the viral life cycle. As a domain within the Gag polyprotein, NC specifically binds and incorporates viral genomic RNA into virions (reviewed in references 5 and 63) and drives virion assembly by promoting interaction among Gag polyproteins (4, 11, 14, 17a, 28, 34, 42, 54, 67). Within the nascent virion, after cleavage from the Gag polyprotein, NC coats viral genomic RNA and promotes its maturation into a more stable dimeric form (26, 27, 30, 31). Upon infection of a susceptible target cell, NC contributes to reverse transcription (RT) (1, 2, 39, 49, 59, 62, 68, 71). NC may also facilitate integration of viral DNA into host cell chromosomal DNA, either by facilitating the integrase-mediated strand transfer or by relieving DNA secondary structure, as suggested by in vitro studies (15, 16, 48). It has been difficult to confirm the in vitro effects of NC on integration in vivo since many NC mutations decrease RNA packaging or directly inhibit the efficiency of RT. The effect of these mutations is to limit the yield of viral DNA synthesized after infection to levels too low for meaningful analysis of subsequent events. Recently, however, Moloney murine leukemia virus (M-MuLV) NC mutations have been shown to block a step in the replication cycle that follows nuclear entry of viral DNA, suggesting that NC plays a role in integration in vivo (36).

All of NC's varied functions appear to depend on its ability to bind RNA (for reviews, see references 5, 19, and 63). Both Cys-His boxes and basic residues are determinants of NC's interaction with RNA, the former providing specificity for interaction with viral genomic RNA and the latter providing nonspecific association with nucleic acid (21). Though NC Cys-His boxes have received a great deal of attention, the basic residues, through their nonspecific RNA-binding activity, mediate many of NC's functions, as mutation of human immunodeficiency virus type 1 (HIV-1) NC basic residues can disrupt RNA packaging (6, 17a, 58, 60), virion assembly (17a, 20), and RT (6, 40).

In this study, we report the isolation of a viral revertant of a replication-defective mutant in which two basic residues at the N terminus of HIV-1 NC are replaced by alanine (R10A/K11A). We show that the phenotypic reversion is due to the presence of a second-site compensatory mutation (E21K). Detailed characterization of the R10A/K11A mutant shows that there are multiple defects throughout the viral life cycle, ranging from genomic RNA packaging to integration of viral DNA. Each of the defects is corrected to a considerable extent by the presence of the E21K mutation.

MATERIALS AND METHODS

Plasmid DNAs. The HIV-1 proviral construct R10A/K11A is described elsewhere (17a). This construct, as well as all the proviral constructs used in this study, are chimeric proviral DNAs in which an *Sph*I/*Eco*RV fragment in NL4-3 that spans the NC coding sequence has been replaced by the corresponding fragment of HXB-2 (nucleotides 1443 to 2977, according to reference 57). Mutation E21K was introduced de novo into mutant and wild-type proviral DNAs by

* Corresponding author. Mailing address: Departments of Microbiology and Medicine, Columbia University College of Physicians and Surgeons, 701 W. 168th St., New York, NY 10032. Phone: (212) 305-8706. Fax: (212) 305-0333. E-mail: jl45@columbia.edu.

mutagenic PCR, according to standard procedures and using oligonucleotides 5′-CAATTGTGGCAAAAAAGGCCACACAGCCAG-3′ (nucleotides 1965 to 1994) and 5′-CTGGCTGTGTGGCCTTTTTTGCCACAATTG-3′ (nucleotides 1994 to 1965). The products obtained after mutagenic PCR were digested with *Sph*I/*Apa*I (nucleotides 1443 to 2001) and used to replace the corresponding fragments of R10A/K11A or wild-type proviral DNAs. Fragment sequences were confirmed by dideoxy sequencing.

Cell lines. The human T-lymphocyte cell line Jurkat (69) was maintained in RPMI 1640 supplemented with 10% fetal bovine serum (FBS). Human 293T and HeLa fibroblasts were maintained in Dulbecco modified Eagle medium (DMEM) supplemented with 10% FBS. HeLa-CD4-LTR-β-gal (obtained through the AIDS Research and Reference Reagent Program; catalog no. 1470) were maintained in DMEM supplemented with 10% FBS, 0.2 mg of G418 per ml, and 0.1 mg of hygromycin B per ml; this cell line expresses CD4 and contains a β-galactosidase (β-Gal) gene under the control of HIV-1 long terminal repeat (LTR) (45).

Viral replication assay. Viral infections were initiated in 10^6 Jurkat cells by DEAE-dextran (250 μg/ml; Pharmacia Biotech Inc., Piscataway, N.J.), using 2 μg of proviral DNA in 1 ml of serum-free RPMI 1640 for 20 min at room temperature. Cells were then washed in serum-free medium and resuspended in 3 ml of conditioned medium. Every 2 days supernatant was harvested and frozen, and cells were passaged. At the conclusion of the experiment, the stored samples were analyzed for exogenous RT activity as described below.

Exogenous RT assay. Cell culture supernatant (10 μl) was added to 50 μl of RT cocktail {60 mM Tris-HCl (pH 8.0), 180 mM KCl, 6 mM $MgCl_2$, 6 mM dithiothreitol (DTT), 0.6 mM EGTA, 0.12% Triton X-100, 6 μg of oligo(dT) and 12 μg of poly(rA) per ml, 0.05 mM [α-^{32}P]dTTP (800 Ci/mmol)} for 1 h at 37°C; 2 μl was spotted onto DEAE-81 paper and washed three times with 2× SSC (1× SSC is 0.15 M NaCl plus 0.015 M sodium citrate) (64). A PhosphorImager (Molecular Dynamics, Sunnyvale, Calif.) was used to quantify the radioactivity incorporated.

Molecular cloning of an R10A/K11A revertant. RNA was extracted from 100 μl of supernatant containing revertant virions at the peak of infection, using an RNAzol B isolation kit (Tel-Test Inc., Friendswood, Tex.) as instructed by the manufacturer. RNA was reverse transcribed for 1 h at 37°C using 200 ng of random primers (Stratagene, La Jolla, Calif.), 20 U of RNAsin inhibitor, 40 U of M-MuLV reverse transcriptase (Gibco-BRL, Rockville, Md.), 50 mM Tris-Cl (pH 8.3), 40 mM KCl, 6 mM $MgCl_2$, 1 mM DTT, and 260 μM deoxynucleoside triphosphates (dNTPs) in a total volume of 30 μl. One-tenth of the RT reaction was amplified using *Pfu* DNA polymerase (Stratagene, La Jolla, Calif.) and primers specific for the *gag* region: 5′-ATGGGTGCGAGAGCGTCGG-3′ (nucleotides 788 to 806) and 5′-CTTTATTGTGACGAGGGGTCGC-3′ (nucleotides 2291 to 2270). PCR products were blunt cloned into pBluescript that had been linearized with *Eco*RV.

Metabolic labeling and immunoprecipitation. HeLa cells in 35-mm-diameter plates were transfected with proviral DNAs by using calcium phosphate as previously described (17a). Forty-eight hours posttransfection, cells were incubated for 1 h at 37°C with 2 ml of DMEM lacking methionine and cysteine prior to a 45-min pulse with 100 μCi of [^{35}S]Met/Cys (Translabel; ICN) in 500 μl. Cells were washed with phosphate-buffered saline (PBS), incubated with complete DMEM, and lysed 0, 1, 3, and 6 h later in radioimmunoprecipitation assay (RIPA) buffer (150 mM NaCl, 1% NP-40, 0.5% deoxycholate, 0.1% sodium dodecyl sulfate [SDS], 50 mM Tris-Cl [pH 8.0]). Virions were purified from the supernatant by ultracentrifugation for 2 h at 80,000 × *g* through a cushion of 25% sucrose (wt/vol); the pellet was resuspended in RIPA buffer. Cell lysate- and virion-associated fractions were incubated with 100 μl of protein A-Sepharose beads (Sigma; 10% slurry in RIPA buffer) for 1 h at 4°C. Supernatant was removed from the beads and incubated with 25 μg of total immunoglobulin from an HIV-1-infected individual (serum obtained from the AIDS Research and Reference Reagent Program; catalog no. 3957) for 2 h at 4°C. Protein A-Sepharose beads (100 μl) were then added for 1 h at 4°C. Beads were washed three times, and proteins bound to the beads were analyzed by SDS-polyacrylamide gel electrophoresis (PAGE) and PhosphorImager quantification.

Analysis of HIV-1 virion morphology by electron microscopy. Jurkat cells were transfected with HIV-1 proviral DNAs, and the infections were allowed to proceed for 14 days. Cells were then fixed with freshly made 2.5% glutaraldehyde in phosphate buffer (pH 7.0). Cells were postfixed in 1% osmium tetroxide and then embedded in Epon. Poststaining was done with 1% uranyl acetate. Sections were cut approximately 60 nm thick to accommodate the volume of the core structure parallel to the section plane. Specimens were analyzed with a Zeiss CEM 902 electron microscope, equipped with a spectrometer to enhance image contrast, at an accelerating voltage of 80 kV. A liquid nitrogen-cooling trap of the specimen holder was used throughout. For each mutant, a series of electron micrographs was used for the statistical evaluation of the classes of different morphology present in the sample; 90 to 300 particles were evaluated for each sample.

Dot blot analysis. Dot blot analysis was performed as previously described (17a). Briefly, virions produced by calcium phosphate transfection of 293T cells were purified by ultracentrifugation through 25% sucrose (wt/vol), resuspended, and normalized by exogenous RT activity. Virions were then transferred to a nylon membrane using a dot blot apparatus (Bio-Rad). The membrane was hybridized overnight at 42°C in 10% polyethylene glycol, 1.5× SSPE (1× SSPE is 0.18 M NaCl, 10 mM NaH_2PO_4, and 1 mM EDTA [pH 7.7]), 7% SDS, 100 μg of salmon sperm DNA per ml with a ^{32}P-end-labeled DNA oligonucleotide (5′-CTGACGCTCTCGCACCC-3′, antisense nucleotides 808 to 792 from pNL4-3) that hybridizes with HIV-1 genomic RNA (53). The membrane was washed in 0.1% SDS–0.2× SSC and analyzed with a PhosphorImager.

Endo-RT assay. Endogenous RT (endo-RT) reactions were performed as previously described (35). Briefly, particles in supernatant obtained from transfection of four 293T cell plates (100-mm diameter) were purified by ultracentrifugation through 25% sucrose at 80,000 × *g* as previously described (17). Virions were resuspended in PBS for 12 to 18 h on ice and normalized by exogenous RT assay. Virions thus normalized were permeabilized by addition of 5 mM β-octylglucoside for 10 min at room temperature. After the permeabilization step, the reaction mixture was made 50 mM Tris-HCl (pH 8.4), 2 mM DTT, 2 mM magnesium acetate, 0.1 mM each dATP, dGTP, and dCTP, and [^{32}P]TTP (12 Ci/mmol) and incubated overnight at 37°C in a total volume of 100 μl. Samples were then treated for 1 h at 55°C with 0.5% SDS, 25 mM EDTA, 100 mM NaCl, tRNA (50 μg/ml), and proteinase K (20 μg/ml), phenol extracted, and ethanol precipitated. Samples were denatured in 0.3 M NaOH for 30 min at 37°C and run on a 1% agarose gel. The gel was dried and exposed for PhosphorImager analysis.

Real-time PCR analysis. Infections were performed as previously described (9). Jurkat cells (10^6) were infected in a total volume of 200 μl of RPMI 1640 for 1 h at 37°C. Medium, was added and cells were incubated 12 h at 37°C. Cell lysis for the isolation of low-molecular-weight DNA was performed as previously described (9, 40). A portion (1/15) of each DNA preparation was amplified in triplicate using 1× TaqMan buffer A (Perkin-Elmer, Norwalk, Conn.), 3.5 mM $MgCl_2$, molecular beacon (0.4 pmol/μl), primer (0.4 pmol/μl), and 1.25 U of AmpliTaq Gold DNA polymerase (Perkin-Elmer) in a total volume of 50 μl. The sequence of molecular beacon (50) is 5′-FAM-GCGGGTTCTGAGGGATCTCTAGTTACCAGACCCGC-DABCYL-3′ (underlined sequence corresponding to nucleotides 9675 to 9653), where 6-carboxyfluorescein (FAM) serves as the reporter fluorochrome and 4-dimethylaminophenylazobenzoic acid (DABCYL) serves as the quencher. This molecular beacon recognizes both full-length proviral DNA and 2-LTR circles. One cycle of denaturation (95°C for 10 min) was followed by 45 cycles of amplification (95°C for 15 s, 60°C for 30 s, and 72°C for 30 s). PCR was carried out in a spectrofluorometric thermal cycler (ABI PRISM 7700; Applied Byosystem Inc.) that monitors changes in the fluorescence spectrum of each reaction tube during the annealing phase while simultaneously carrying out programmed temperature cycles. PCR primer pairs used to specifically amplify full-length proviral DNA and 2-LTR circles were 5′-GCTAGTACCAGTTGAGCCAGATAAG-3′ (nucleotides 9215 to 9239) plus 5′-AGCAAGCCGAGTCCTGCGTC-3′ (nucleotides 705 to 686) and 5′-GGTACTAGCTTGAAGCACCATCC-3′ (nucleotides 149 to 127) plus 5′-GCCTCAATAAAGCTTGCCTTGAGTG-3′ (nucleotides 9594 to 9618), respectively. Each sample was normalized as described above with primers and beacon specific for mitochondrial DNA (accession no. J01415): 5′-CACAGCCACTTTCCACACAGACAT-3′ (nucleotides 257 to 280), 5′-GATGCGATTAGTAGTATGGGAGTGGG-3′ (nucleotides 485 to 459), and 5′-FAM-GCGCGGTGGGGTTTGGCAGAGATGTGCCGCGC-DABCYL-3′ (underlined sequence corresponding to nucleotides 357 to 337).

Single-round infectivity assay. HeLa-CD4-LTR-β-gal cells (45) were seeded 24 h before infection at 40,000 cells/well (12-well plate) in medium lacking drug for selection. Infection was performed in 500 μl with DEAE-dextran (15 μg/ml). Two hours postinfection, 1 ml of DMEM was added. After 2 days, cells were washed with PBS and fixed with a freshly made solution of 1% formaldehyde–0.2% glutaraldehyde in PBS for 5 min at room temperature. Cells were again washed with PBS and incubated with 1 ml of 4 mM potassium ferrocyanide, 4 mM potassium ferricyanide, 1 mM $MgCl_2$, and 0.4 mg of 5-bromo-4-chloro-3-indolyl-β-D-galactopyranoside (X-Gal) per ml in PBS for 50 min in a non-CO_2 incubator. Cells were washed in PBS, and β-Gal-positive cells were counted in an optic microscope.

Computer modeling of NC structure. Three-dimensional coordinates for the nuclear magnetic resonance structure of NC complexed with the SL3-RNA (21) were retrieved from the National Center for Biotechnology Information database (PBD Id:1A1T). Graphical display of the data was generated by using the computer software program Insight II (Biosym/Molecular Simulation).

RESULTS

Isolation of a phenotypic revertant of the R10A/K11A mutant. Previous studies demonstrated that mutation of multiple basic residues in HIV-1 NC generally impairs viral replication in T-lymphocyte cell lines (17a, 60). In an attempt to obtain phenotypic viral revertants of such mutants, five viral DNAs bearing different NC mutations were each transfected individually into Jurkat T cells. These viral mutants ranged in severity from 2 to 10 basic residues substituted with alanine (17a). After 60 days of passage, RT activity was detected in the supernatant of Jurkat cells that had been transfected with the

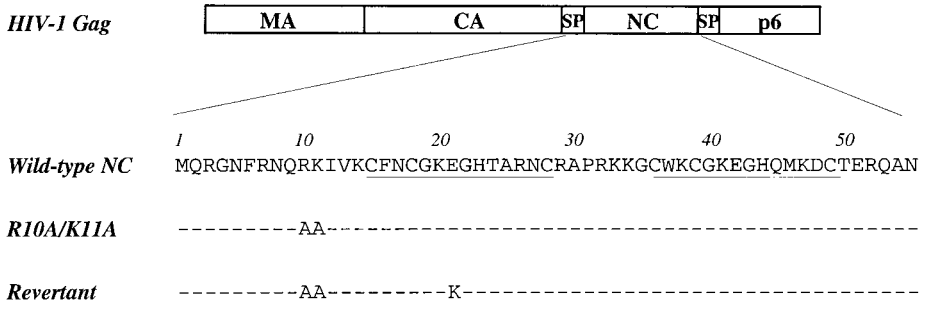

FIG. 1. Schematic representation of the major domains of the HIV-1 Gag polyprotein. Amino acid sequences of wild-type and mutant NC proteins are given below. Dashes indicate amino acid identity with the wild type. Cys-His boxes are underlined. MA, matrix; SP, spacer.

R10A/K11A HIV-1 proviral DNA construct (Fig. 1). No other culture yielded evidence of viral replication. To determine if the increase in exogenous RT activity was due to the emergence of a phenotypic revertant, supernatant from this cell culture was used to infect fresh Jurkat cells. Upon retesting, virus grew with wild-type kinetics, suggesting the presence of a revertant virus (data not shown).

A second-site suppressor mutation (E21K) is sufficient to rescue replication of the R10A/K11A mutant. To determine the genetic basis for phenotypic reversion, the entire *gag* coding sequence was analyzed. Viral genomic RNA was extracted from virions, reverse transcribed, and amplified by PCR using primers that allowed amplification of the entire *gag* gene. The PCR product was ligated into a plasmid, and the complete *gag* coding sequences of several individual clones were determined. All clones contained the original R10A/K11A NC mutation, indicating that phenotypic reversion was not explained by a reversion mutation or by contamination with wild-type virus. One clone contained a silent mutation in CA (data not shown). A second-site mutation in NC (E21K) was present in all clones (Fig. 1), suggesting that we had identified the genetic basis for phenotypic reversion.

To determine if the second-site mutation in NC was responsible for the observed phenotypic reversion, the E21K mutation was introduced de novo into both wild-type and R10A/K11A mutant proviral DNA constructs. Jurkat T cells were transfected with the proviral DNAs. Supernatant was collected every 2 days, and exogenous RT activity was determined as an indication of viral spread through the culture (Fig. 2). As expected, no detectable exogenous RT activity was measured in the supernatant of Jurkat cells transfected with the R10A/K11A proviral DNA construct. In contrast, exogenous RT activity accumulated with the same kinetics as the wild type when cells were transfected with either R10A/K11A/E21K or E21K proviral DNA. These results prove that the E21K mutation is sufficient to correct the replication defect of mutant R10A/K11A.

Analysis of virion assembly kinetics. Since NC plays roles in practically all steps of the retroviral life cycle, we examined the effect of the R10A/K11A double mutation and of the R10A/K11A/E21K triple mutation on each of these steps. The effect of R10A/K11A on viral replication has been partially characterized elsewhere (17a, 60). A decreased efficiency of virion release and the accumulation of incompletely processed p25 (consisting of CA [capsid protein] fused to the spacer peptide) has been found with R10A/K11A (17a). To determine if virion assembly of R10A/K11A was rescued by the E21K mutation, HeLa cells were transfected with wild-type and R10A/K11A/E21K proviral DNAs and pulsed for 45 min with [^{35}S]Met/Cyst (Fig. 3). Labeled proteins were chased for 0, 1, 3, and 6 h, and cell-associated and virion-associated proteins were immunoprecipitated with serum from an HIV-1-infected individual. Mutant R10A/K11A/E21K assembled virions with kinetics similar to that of the wild type (Fig. 3), with normal accumulation of Gag-processing intermediates. The magnitude of virion release was determined to be near normal when the virion-associated CA signal at the 6-h time point was normalized to the intensity of the cell-associated Gag polyprotein signal at the 0-h time point (Table 1). These results demonstrated that the defect in viral assembly of mutant R10A/K11A was corrected by the second-site mutation E21K. Expression and processing of *env*-encoded proteins was normal. Also, processing of *gag*- and *pol*-encoded proteins at other sites appeared normal, as judged by Western blot analysis (data not shown).

Morphology of NC mutant virions. Infection of Jurkat cells was initiated by transfection of proviral DNAs; after 14 days, cells were fixed and analyzed by electron microscopy. As expected, the majority (96%) of wild-type virions exhibited mature, cone-shaped core structures of high density (Fig. 4a); 3% of wild-type particles exhibited immature morphology with a

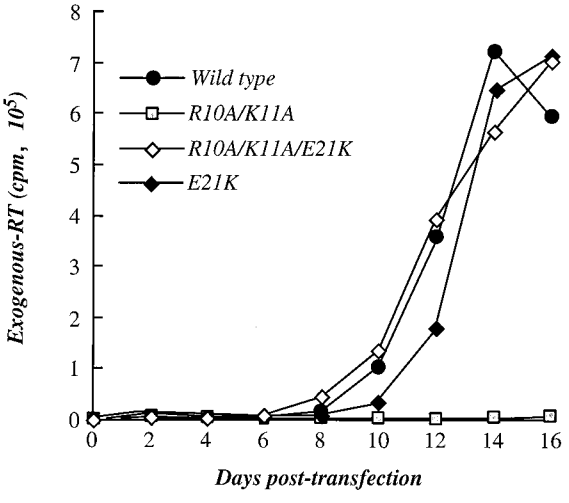

FIG. 2. Replication of HIV-1 wild type and NC mutants following transfection of proviral DNAs into the Jurkat T-cell line. The accumulation of RT activity in the cell culture supernatant (ordinate) is shown for the indicated day posttransfection (abscissa).

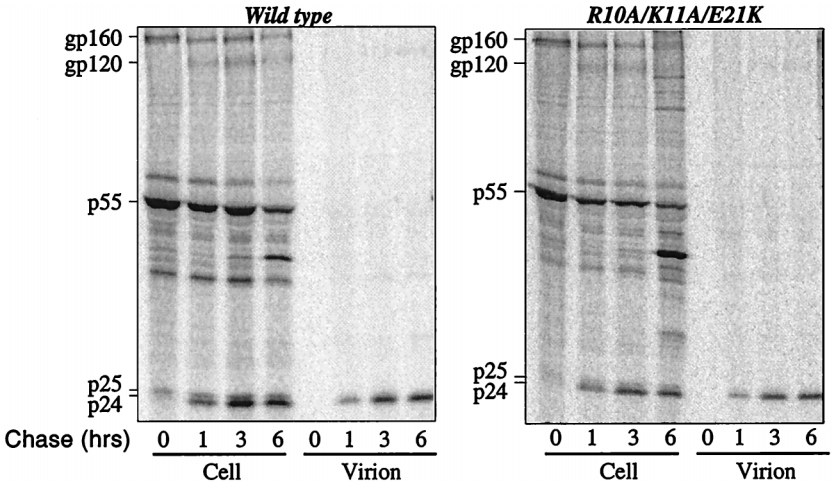

FIG. 3. Pulse-chase analysis of HIV-1 NC wild type and R10A/K11A/E21K mutant. HeLa cells transfected with the indicated proviral DNAs were metabolically labeled with [^{35}S]Met/Cys for 45 min and chased for 0, 1, 3, 6 h, as indicated. Virion-associated proteins were purified by ultracentrifugation through 25% sucrose. Virion- and cell-associated proteins were immunoprecipitated with sera from an HIV-1-infected individual and analyzed by SDS-PAGE. Positions of mobility of the envelope glycoprotein precursor (gp160), surface envelope protein (gp120), Pr55^{Gag} precursor (p55), incompletely processed Gag precursors (p41 and p25), and completely processed CA (p24) are indicated on the left.

rim of high-density material inside the envelope, and 1% exhibited an irregular core structure. The majority of particles (79%) observed with the R10A/K11A mutant were immature, with a characteristic rim of high-density material present inside the envelope (Fig. 4b); 2% of these virions had a dense, globular core structure in the center.

Consistent with the restored replicative capacity conferred by the second-site suppressor mutation, 85% of R10A/K11A/E21K virions exhibited a mature morphology with cone-shaped core structures of high density (Fig. 4d). In addition, 13% of virion particles contained two globular core structures of high density (Fig. 4c); 2% of the R10A/K11A/E21K virions exhibited a dense, globular core structure in the center.

When virions were produced by provirus bearing only the E21K mutation in an otherwise wild-type background, 89% exhibited the morphology of normal, mature virions (Fig. 4f), and 3% had a dense, globular core structure in the center (Fig. 4e). Interestingly, 8% had two or as many as four core structures of high density (Fig. 4g).

Effect of the second-site compensatory mutation on viral genomic RNA incorporation into virions. Viral genomic RNA incorporation has been shown to be modestly impaired in R10A/K11A virions ((17a, 60). To determine if the second-site mutation restored viral genomic RNA incorporation to normal levels, virions produced by transfection of 293T cells with wild-type, R10A/K11A, or R10A/K11A/E21K proviral DNAs were purified and normalized by exogenous RT activity. The amount of viral genomic RNA incorporated was then determined by dot blot analysis as previously described (17a, 52). Supernatant obtained from cells transfected with proviral DNA coding for a myristylation-deficient Gag was used as a negative control. The R10A/K11A mutation reduced RNA packaging to levels 22% of that of the wild-type (Fig. 5 and Table 1) (17a, 60). The presence of the second-site mutation (R10A/K11A/E21K) increased the amount of viral genomic RNA incorporated into virions by approximately threefold compared to the R10A/K11A mutant (Fig. 5 and Table 1).

Effect of the second-site mutation on endo-RT. To determine if impairment in viral replication was due to an intrinsic defect in the RT reaction, endo-RT was examined next. Purified virions were permeabilized with 5 mM β-octylglucoside and incubated for 24 h at 37°C with unlabeled dNTPs plus [^{32}P]TTP. Virions were then treated with proteinase K, and nucleic acid was extracted and precipitated. Samples were then run on an agarose gel. A band corresponding to full-length viral DNA was observed in wild-type and both mutant virions (Fig. 6). We also observed a smear, containing degradation products and incomplete forms of RT (8, 35, 44), constituting up to 90% of the total radioactivity present in the lanes. Because of the smear, we considered quantitation of the results relatively inaccurate, but a decrease (about threefold) in the overall amount of endo-RT products was observed in R10A/K11A virions relative to the wild type. For the R10A/K11A/E21K mutant, the reduction in endo-RT product was slightly less (about twofold). Similar results were obtained when virion permeabilization was performed with 0.01% Triton X-100 (data not shown).

Quantitation of viral DNA synthesis after infection using real-time PCR. The effect of the NC mutations on the early steps of the viral life cycle was studied by quantifying full-length linear viral DNA and 2-LTR circles synthesized after a single round of infection using real-time PCR. Virions normalized by exogenous RT were used to infect Jurkat T cells. Low-molecular-weight DNA was harvested 12 h postinfection. PCR was performed with primer pairs that amplify full-length linear DNA or 2-LTR circles. By exploiting nucleotide differences between the 5′ and 3′ LTRs of pNL4-3, the primers amplify only newly synthesized viral DNA and not contaminating plasmid DNA carried over from the transfection in which the virions were produced (9). To ensure that there were equal amounts of sample DNA added to each real-time PCR, mitochondrial DNA was amplified with specific primers (9) and quantitated as described below with a molecular beacon (see Materials and Methods for details).

To quantify the viral DNA template copy number in each sample, a molecular beacon was used in combination with real-time PCR as previously described (46, 50). The molecular beacon is an oligonucleotide with a fluorochrome at one end and a quencher at the other. It is designed to form a stem-loop structure that brings the quencher in close proximity to the fluorochorome. As a result, little signal is emitted when the beacon is in its folded conformation. The loop is designed to

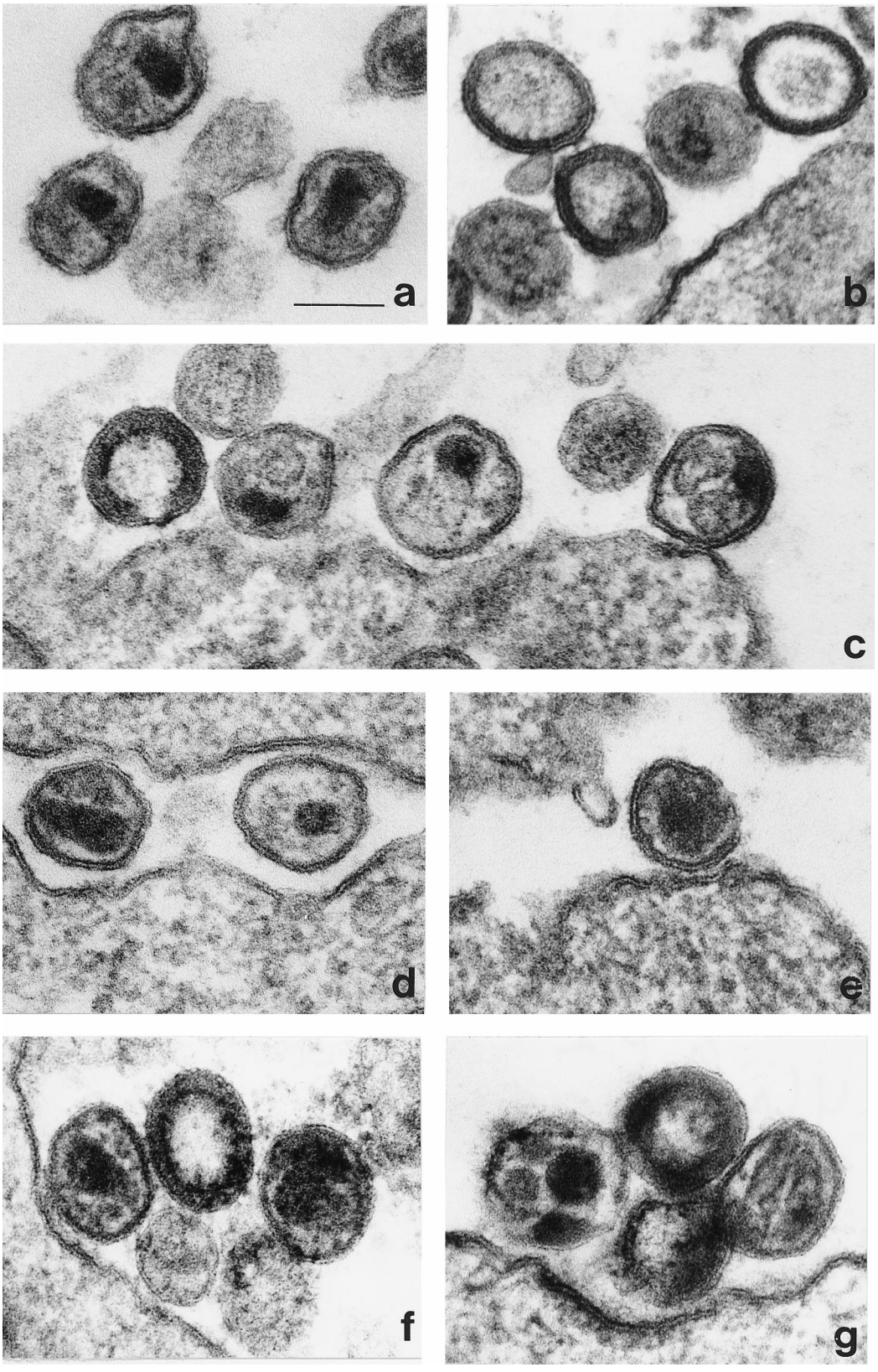

FIG. 4. Analysis of virion morphology by electron microscopy. Jurkat cells were transfected with proviral DNAs; 14 days later, cells were fixed, stained, embedded, and visualized by electron microscopy. (a) Mature wild-type virions showing a characteristic cone-shaped core structure of high density. (b) Virus particles of mutant R10A/K11A showing a rim of high-density material inside the envelope and occasionally a dense, globular core structure in the center. (c) Particles of mutant R10A/K11A/E21K showing a rim of high-density material inside the envelope (left) and two globular core structures (left, middle, and right). (d) Particles of mutant R10A/K11A/E21K showing a cone-shaped core structure of high density (left). (e) Particle of mutant E21K showing a dense, globular core structure in the center. (f) Mutant E21K virions showing a cone-shaped core structure of high density (left), a rim of high-density material inside the envelope (middle), and two core structures of high density (right). (g) Particles of mutant E21K showing two extended core structures of low density (right), two to four globular core structures of high density (left), and a rim of high-density material inside the envelope (middle). The bar indicates 100 nm.

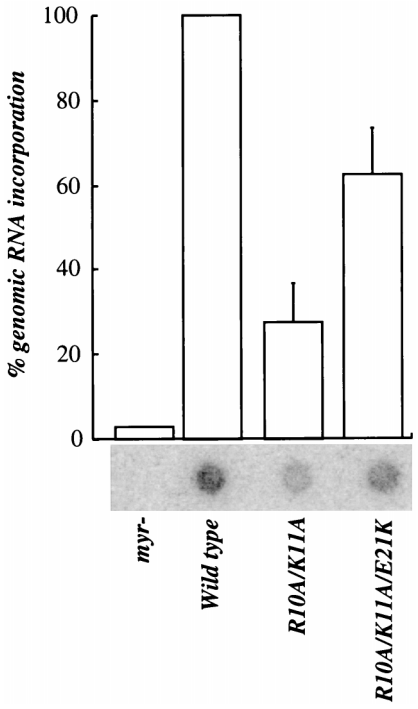

FIG. 5. Viral genomic RNA incorporation into wild-type and mutant virions. Virions produced by transfection of 293T cells with proviral DNAs were purified by ultracentrifugation through 25% sucrose, resuspended in PBS, and normalized by exogenous RT assay. Normalized amount of virions were loaded onto a nylon membrane and probed with a ^{32}P-end-labeled DNA oligonucleotide specific for viral genomic RNA. The signal obtained after hybridization was quantified with a PhosphorImager. Results are presented as percentage of wild-type virus activity. The bar graph presents results obtained from three independent experiments with standard errors of the mean (primary data from a representative experiment are shown underneath). *myr*$^-$ indicates a virion preparation from cells transfected with a myristylation-deficient NL4-3.

hybridize with the amplified sequence, so that at each annealing step, the molecular beacon anneals to the amplified sequences. Consequently, with each PCR cycle increasing fluorescence is emitted that is detected by a spectrofluorometric thermal cycler (ABI PRISM 7700; Applied Biosystems Inc.).

For each experiment, a standard curve was generated by experimentally determining the threshold cycle (C_T) for known template DNA copy number (in duplicate) ranging from 10 to 10^6 molecules. C_T is the cycle number at which the mean fluorescence rises 10 standard deviations above the baseline. For either the full-length linear DNA (Fig. 7A) or the 2-LTR circles (data not shown), the C_T was directly proportional to the template input copy equivalents (Fig. 7A, inset).

Copy number for each experimental sample was calculated by interpolation from the experimentally determined C_T standard curve. At 12 h postinfection, the steady-state level of full-length proviral DNA with mutant R10A/K11A was 10% of the wild-type level (Fig. 7B and Table 1). Considering the method that we used for normalizing virions, and correcting for the fivefold reduction in RNA packaging, the actual defect in RT with R10A/K11A was only twofold. An identical defect was observed in the formation of 2-LTR circles by the R10A/K11A mutant (Fig. 7C), suggesting that there was no measurable defect in nuclear import of the preintegration complex. R10A/K11A/E21K accumulated nearly wild-type levels of both full-length linear and 2-LTR DNAs (Fig. 7B and C).

Effect of NC mutants in the MAGI assay. An indicator cell line, HeLa-CD4-LTR-β-gal, bearing a β-Gal gene under the control of the HIV-1 LTR (45), was used to determine the infectivity of mutant virions in a single round of infection. Virions produced by transfection of 293T cells were purified by ultracentrifugation through 25% sucrose, resuspended, and normalized by exogenous RT activity. Normalized virions were used to infect HeLa-CD4-LTR-β-gal cells in triplicate. Two days postinfection, cells were washed and fixed in formaldehyde, and β-Gal-positive cells were counted.

Cells infected with different dilutions of virion stocks indicated that the R10A/K11A mutant had 100-fold-lower titer than the wild type (Fig. 8). A 100-fold relative decrease in titer associated with the R10A/K11A mutation was observed whether the experiment was performed with virus stocks generated by transfection with complete provirus (Fig. 8) or with *env*-deleted proviruses pseudotyped with vesicular stomatitis virus G protein (VSV-G) (data not shown). This indicates that the observed β-Gal activity was due to a single round of viral infection. Similar results were obtained when, instead of measuring β-Gal activity, we measured luciferase activity after infection with a VSV-G-pseudotyped virus in which *env* had been replaced with a luciferase gene cassette (data not shown). Since full-length viral DNA and 2-LTR circles were decreased 10-fold with the R10A/K11A mutant, these results indicate that there is at least an additional 10-fold reduction in infectivity due to disruption of postnuclear import processes such as integration. As judged by the MAGI assay, the second-site mutation restored the infectivity of mutant R10A/K11A/E21K virions almost to wild-type levels (42%).

DISCUSSION

In this report we have described the detailed characterization of HIV-1 NC mutant R10A/K11A and of a phenotypic

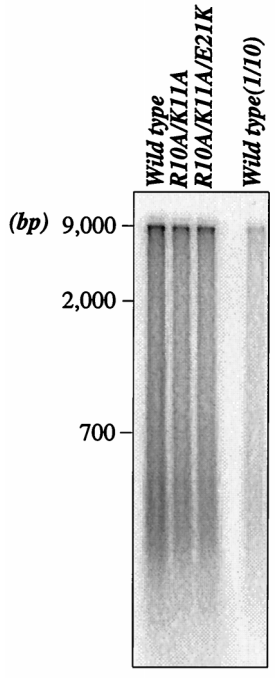

FIG. 6. Endo-RT in wild-type and mutant virions. After purification through 25% sucrose and normalization by exogenous RT, virions produced by transient transfection of 293T cells were permeabilized with β-octylglucoside and incubated with [^{32}P]TTP and unlabeled dNTPs. The products of endo-RT were extracted with proteinase K, precipitated, and run on an agarose gel prior to PhosphorImager analysis.

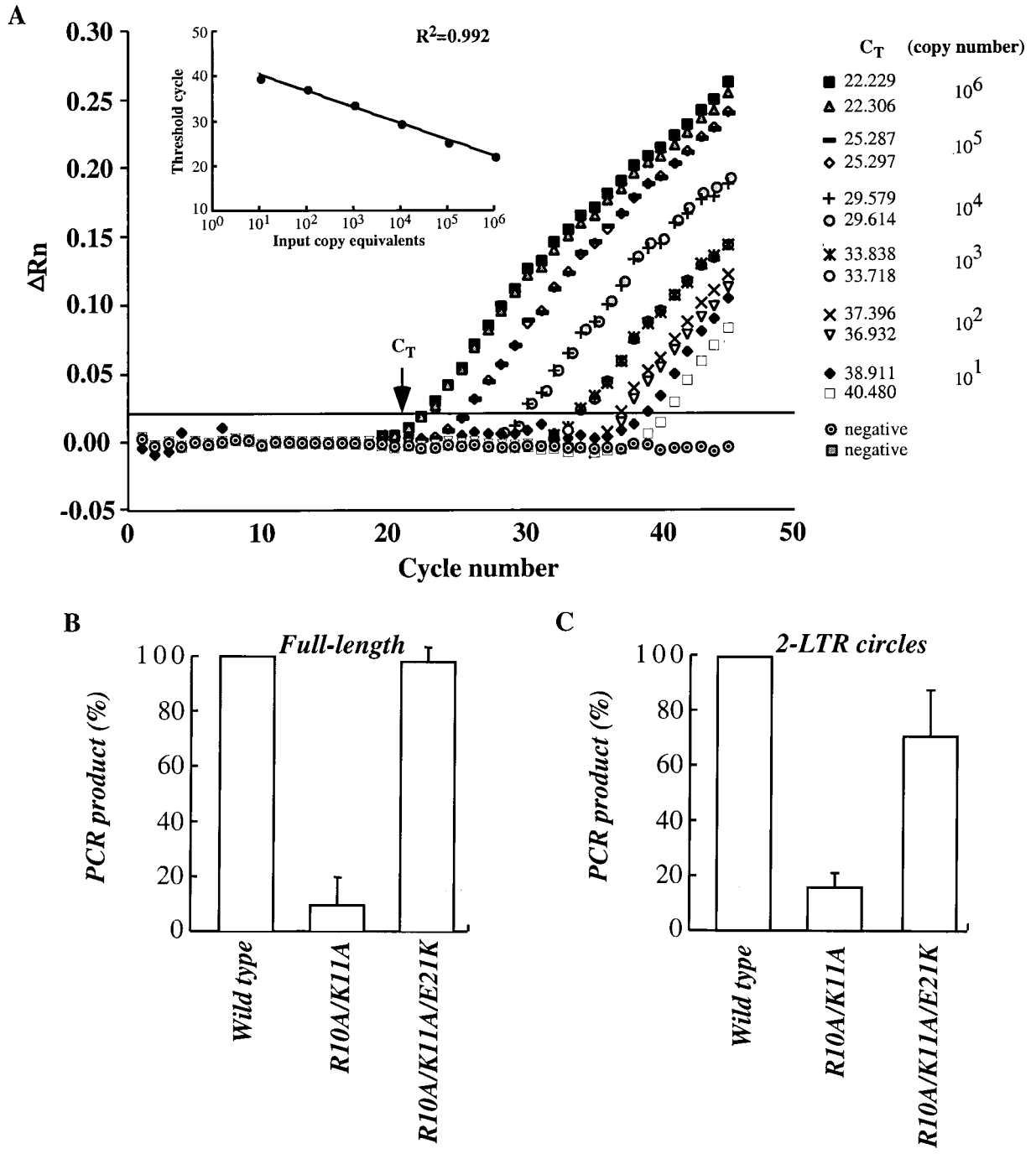

FIG. 7. Quantitation of steady-state viral DNA 12 h after infection of Jurkat T cells. (A) Representative standard curve for the quantitation of full-length viral DNA sequences using real-time PCR with a molecular beacon. Change in fluorescence (ΔRn) as a function of cycle number is demonstrated for viral DNA plasmid copy numbers ranging from 10 to 10^6 per reaction. The C_T is shown for duplicates of the standards used. The inset shows the relationship between known input DNA copy numbers and the C_T. The C_T is directly proportional to the log of the input copy equivalents, as demonstrated by the standard curve generated ($r^2 = 0.992$). (B and C) Low-molecular-weight DNA was isolated from Jurkat cells after infection with the indicated viruses (9, 40). Real-time PCR was performed using primers specific for full-length (B) or circular 2-LTR (C) viral DNA. Input copy number was determined as shown in panel A. Results are presented as percentage of wild-type viral DNA. The bar graph presents results obtained from two independent experiments with standard errors of the mean.

revertant bearing a second-site suppressor mutation (R10A/K11A/E21K). Given the many roles of NC in the retrovirus life cycle, we examined the effect of our mutants on steps spanning the entire replication cycle. By this approach, we demonstrated that mutant R10A/K11A exhibits several, distinct defects, the major ones being in integration and RNA packaging.

A defect in viral RNA packaging and virion assembly has been previously reported for mutant R10A/K11A (17a, 60).

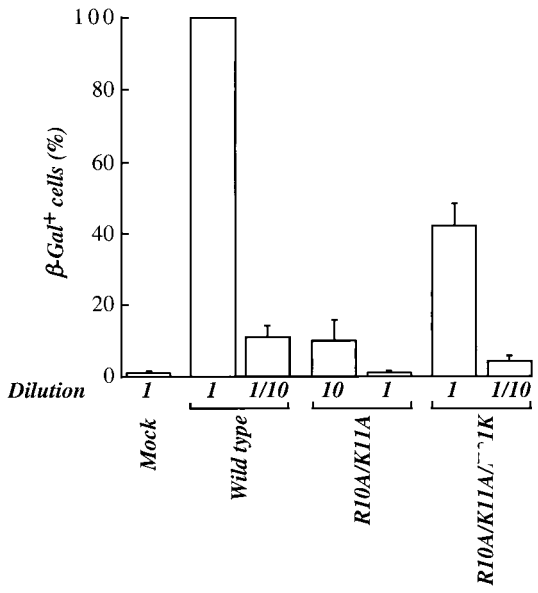

FIG. 8. Infectivity of HIV-1 wild-type and NC mutant virions after a single-round infection (MAGI assay). Virions produced by transfection of proviral DNAs into 293T cells were purified by ultracentrifugation through 25% sucrose. Virions were normalized by exogenous RT and used to infect HeLa-CD4-LTR-β-gal cells. Cells were infected with the indicated amounts of wild-type and mutant virion preparations. Infectious titers were determined by scoring the number of β-Gal-positive cells 2 days postinfection. Results are presented as percentage of wild-type virus activity. The bar graph presents results obtained from three independent experiments with standard errors of the mean.

These defects were corrected in the revertant, although the level of RNA packaging in R10A/K11A/E21K virions was still only 60% of the wild-type level. In addition, a Gag-processing defect present in mutant R10A/K11A (17a) was also corrected in R10A/K11A/E21K virions. The biochemical analysis was supported by electron microscopy analysis showing that R10A/K11A/E21K virions had wild-type morphology, while R10A/K11A virions showed lack of core condensation, also as previously reported (17a, 60).

Though the majority have immature morphology, R10A/K11A mutant virions were still able to infect target cells and to complete RT. The efficiency of RT was accurately quantitated using real-time PCR and found to be 10-fold lower in mutant R10A/K11A than in the wild type or R10A/K11A/E21K. However, the actual magnitude of the RT defect is much less, given that R10A/K11A mutant virions are impaired for RNA packaging and therefore contain less template for DNA synthesis. Indeed, in our assays, virions were normalized for protein content and do not account for differences in RNA packaging.

TABLE 1. Summary of results obtained with HIV-1 NC mutants

Mutant	Replication	% of wild-type value			
		Virion assembly	Viral genomic RNA packaging[a]	Single-round infection[a]	
				PCR; full length	MAGI assay
R10A/K11A	−	33[b]	22	10	1
R10A/K11A/E21K	+	68	62	98	42

[a] Adjusted for virion assembly defect.
[b] From reference 17a.

If one corrects the results obtained by real-time PCR for the amount of viral genomic RNA packaged into mutant virions, the reduction in DNA synthesis by mutant R10A/K11A is only twofold compared to the wild-type level. Thus, mutant R10A/K11A virions infect cells and reverse transcribe to quasi-wild-type levels. This finding is in agreement with the observation that endo-RT is essentially normal in our mutants, and it also suggests that $tRNA_3^{Lys}$ placement and dimeric RNA formation are not affected in our NC mutant.

Formation of 2-LTR circles was found to be reduced to the same extent as full-length viral DNA, suggesting that nuclear import of the preintegration complex (PIC) occurs normally in cells infected with the R10A/K11A mutant. 2-LTR circles are not believed to be substrates for integration (10, 18, 23, 43, 51) but are considered markers of successful nuclear important because they result from ligation of full-length viral DNA by cellular DNA ligases that localize in the nucleus (3, 24, 65, 66, 70). Our quantitation of 2-LTR circles was performed with dividing Jurkat T cells, and so it remains possible that a nuclear import defect would be detected after infection of a nondividing cell such as a macrophage.

Since RT and nuclear import in Jurkat T cells are hardly affected in the R10A/K11A mutant, a defect in a subsequent step must be invoked to explain the 100-fold reduction in infectivity in MAGI assays (or at least a 10-fold reduction if one considers the 5-fold packaging defect and 2-fold RT defect). We believe this defective step to be integration. A role for NC in integration has been proposed based on in vitro assays (15, 16) and based on the finding that certain NC zinc finger mutants exhibit a defect in vivo, after nuclear translocation of viral DNA (36, 37).

How NC might affect integration is unclear, especially since NC's presence in purified PICs is not agreed on by all investigators (25, 32). NC might act directly on the integration reaction, as recently proposed by others (16), by facilitating DNA condensation and/or DNA melting, conditions that promote integration (7, 12, 56, 61). NC might maintain the integrity of viral DNA; M-MuLV NC mutants have been shown to synthesize 2-LTR circles containing large deletions and insertions at the junctions (36). A limited analysis of the sequence of the 2-LTR circle junctions produced by our R10A/K11A mutant, however, showed no obvious differences from the wild type (data not shown).

Alternatively, the effect of NC on integration might be indirect, being exerted, for example, by regulating viral protease processing of PIC components. The only evidence for a protease processing defect in mutant R10A/K11A is the accumulation of incompletely processed CA, as processing at other sites appears normal (17a). How this would affect integration is unclear, since only traces amounts of CA are found in highly purified PICs, questioning their relevance in the integration process (55). Last, although we believe that mutant R10A/K11A exhibits a defect in integration, it is also possible that our mutant is affected at an as yet uncharacterized step that occurs after nuclear translocation of viral DNA.

The presence of the second-site change E21K compensates for all of the defects that were observed with the R10A/K11A mutation. In the solution structure of wild-type HIV-1 NC complexed with the HIV-1 SL3 stem-loop RNA, NC residues R10 and K11 lie on a 3_{10} helix and contact phosphodiester groups on the RNA (21). Interestingly, residue E21 lies on the same face of NC as R10 and K11, where it contacts residue K14 and is believed to stabilize the first zinc finger (Fig. 9). Requirement for this stabilization must not be absolute, since residue E21 can be mutated in the context of otherwise wild-type proviral DNA without an appreciable defect in virion

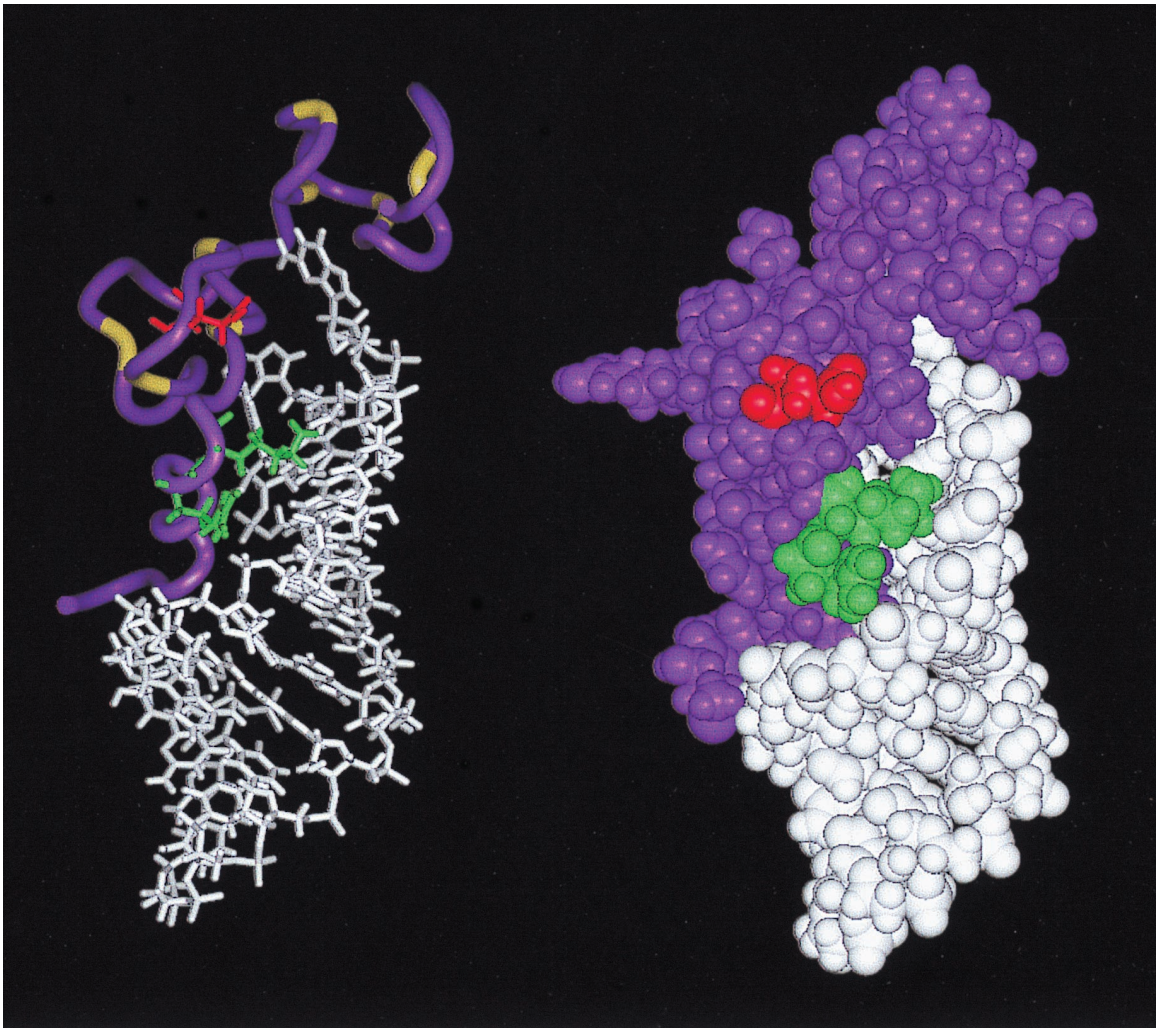

FIG. 9. Ribbon diagram (left) and space-filling image (right) of the HIV-1 NC-SL3 ψ-RNA complex (21). NC is shown in purple. Residues R10/K11 and E21 are shown in green and red, respectively. SL3 RNA is shown in white. Cysteine and histidine residues participating in the two Cys-His boxes are shown in yellow on the left.

replication, in agreement with a previous study (22). However, a significant proportion (~10%) of E21K virions have multiple core structures, and this may be related to a destabilizing effect of the mutation on the first zinc-finger. How an NC mutation would induce the production of virions with multiple cores is unknown. Clearly though, NC is present when the core assembly process is initiated and, interestingly, successful attempts to induce conical core formation in vitro have utilized a Gag fusion protein that encompasses CA and NC (13, 33, 38).

A complete understanding of how E21K rescues R10A/K11A replication will require the determination of the structure of these mutants. The E21K mutation might rescue replication by restoring local positive charge, thus reestablishing contacts with the RNA phosphodiester groups that had been disrupted by the R10A/K11A mutation. Alternatively, the effects of E21K might be less specific and the mutation might simply serve to restore the net positive charge of NC above a critical threshold required for nonspecific RNA binding. The latter possibility seems unlikely given that several HIV-1 NC mutants in which two basic residues are mutated to alanine are able to replicate to wild-type levels (60). In either case, the identification of E21K as a second-site suppressor of R10A/K11A underlines the importance of NC basic residues for HIV-1 replication.

ACKNOWLEDGMENTS

We thank Anna Aldovini for generously providing plasmid DNA. We thank Cagan Gurer for critical reading of the manuscript and Douglas Brateen and Leondios Kostrykis for technical assistance with the real-time PCR. We are indebted to Mohammed Asmal for graphic work.

This work was supported by grant AI 41857 (J.L.) and by shared core facilities of the Columbia-Rockefeller Center for AIDS Research (P30 AI42848), both from the National Institutes of Health, and by contract 975313 from the Swedish Cancer Foundation (S.H.).

REFERENCES

1. **Allain, B., M. Lapadat-Tapolsky, C. Berlioz, and J. L. Darlix.** 1994. Transactivation of the minus-strand DNA transfer by nucleocapsid protein during reverse transcription of the retroviral genome. EMBO J. **13:**973–981.
2. **Allain, B., J. B. Rascle, H. de Rocquigny, B. Roques, and J. L. Darlix.** 1998. CIS elements and trans-acting factors required for minus strand DNA transfer during reverse transcription of the genomic RNA of murine leukemia virus. J. Mol. Biol. **277:**225–235.
3. **Ansari-Lari, M. A., L. A. Donehower, and R. A. Gibbs.** 1995. Analysis of human immunodeficiency virus type 1 integrase mutants. Virology **213:**680.
4. **Bennett, R. P., T. D. Nelle, and J. W. Wills.** 1993. Functional chimeras of the

Rous sarcoma virus and human immunodeficiency virus Gag proteins. J. Virol. **67:**6487–6498.
5. **Berkowitz, R., J. Fisher, and S. P. Goff.** 1996. RNA packaging. Curr. Top. Microbiol. Immunol. **214:**177–218.
6. **Berthoux, L., C. Pechoux, M. Ottmann, G. Morel, and J. L. Darlix.** 1997. Mutations in the N-terminal domain of human immunodeficiency virus type 1 nucleocapsid protein affect virion core structure and proviral DNA synthesis. J. Virol. **71:**6973–6981.
7. **Bor, Y. C., F. D. Bushman, and L. E. Orgel.** 1995. In vitro integration of human immunodeficiency virus type 1 cDNA into targets containing protein-induced bends. Proc. Natl. Acad. Sci. USA **92:**10334–10338.
8. **Borroto-Esoda, K., and L. R. Boone.** 1991. Equine infectious anemia virus and human immunodeficiency virus DNA synthesis in vitro: characterization of the endogenous reverse transcriptase reaction. J. Virol. **65:**1952–1959.
9. **Braaten, D., E. K. Franke, and J. Luban.** 1996. Cyclophilin A is required for an early step in the life cycle of human immunodeficiency virus type 1 prior to the initiation of reverse transcription. J. Virol. **70:**3551–3560.
10. **Brown, P. O., B. Bowerman, H. E. Varmus, and J. M. Bishop.** 1987. Correct integration of retroviral DNA in vitro. Cell **49:**347–356.
11. **Burniston, M. T., A. Cimarelli, J. Colgan, S. P. Curtis, and J. Luban.** 1999. Human immunodeficiency virus type 1 Gag polyprotein multimerization requires the nucleocapsid domain and RNA and is promoted by the capsid-dimer interface and the basic region of matrix protein. J. Virol. **73:**8527–8540.
12. **Bushman, F. D., and R. Craigie.** 1992. Integration of human immunodeficiency virus DNA: adduct interference analysis of required DNA sites. Proc. Natl. Acad. Sci. USA **89:**3458–3462.
13. **Campbell, S., and A. Rein.** 1999. In vitro assembly properties of human immunodeficiency virus type 1 Gag protein lacking the p6 domain. J. Virol. **73:**2270–2279.
14. **Carriere, C., B. Gay, N. Chazal, N. Morin, and P. Boulanger.** 1995. Sequence requirements for encapsidation of deletion mutants and chimeras of human immunodeficiency virus type 1 Gag precursor into retrovirus-like particles. J. Virol. **69:**2366–2377.
15. **Carteau, S., S. C. Batson, L. Poljak, J. F. Mouscadet, H. de Rocquigny, J. L. Darlix, B. P. Roques, E. Kas, and C. Auclair.** 1997. Human immunodeficiency virus type 1 nucleocapsid protein specifically stimulates Mg^{2+}-dependent DNA integration in vitro. J. Virol. **71:**6225–6229.
16. **Carteau, S., R. J. Gorelick, and F. D. Bushman.** 1999. Coupled integration of human immunodeficiency virus type 1 cDNA ends by purified integrase in vitro: stimulation by the viral nucleocapsid protein. J. Virol. **73:**6670–6679.
17. **Cimarelli, A., and J. Luban.** 1999. Translation elongation factor 1-alpha interacts specifically with the human immunodeficiency virus type 1 Gag polyprotein. J. Virol. **73:**5388–5401.

17a. **Cimarelli, A., S. Sandin, S. Höglund, and J. Luban.** 2000. Basic residues in human immunodeficiency virus type 1 nucleocapsid promote virion assembly via interaction with RNA. J. Virol. **74:**3046–3057.

18. **Craigie, R., T. Fujiwara, and F. Bushman.** 1990. The IN protein of Moloney murine leukemia virus processes the viral DNA ends and accomplishes their integration in vitro. Cell **62:**829–837.
19. **Darlix, J. L., M. Lapadat-Tapolsky, H. de Rocquigny, and B. P. Roques.** 1995. First glimpses at structure-function relationships of the nucleocapsid protein of retroviruses. J. Mol. Biol. **254:**523–537.
20. **Dawson, L., and X. F. Yu.** 1998. The role of nucleocapsid of HIV-1 in virus assembly. Virology **251:**141–157.
21. **De Guzman, R. N., Z. R. Wu, C. C. Stalling, L. Pappalardo, P. N. Borer, and M. F. Summers.** 1998. Structure of the HIV-1 nucleocapsid protein bound to the SL3 psi-RNA recognition element. Science **279:**384–388.
22. **Dorfman, T., J. Luban, S. P. Goff, W. A. Haseltine, and H. G. Gottlinger.** 1993. Mapping of functionally important residues of a cysteine-histidine box in the human immunodeficiency virus type 1 nucleocapsid protein. J. Virol. **67:**6159–6169.
23. **Ellis, J., and A. Bernstein.** 1989. Retrovirus vectors containing an internal attachment site: evidence that circles are not intermediates to murine retrovirus integration. J. Virol. **63:**2844–2846.
24. **Engelman, A., G. Englund, J. M. Orenstein, M. A. Martin, and R. Craigie.** 1995. Multiple effects of mutations in human immunodeficiency virus type 1 integrase on viral replication. J. Virol. **69:**2729–2736.
25. **Farnet, C. M., and F. D. Bushman.** 1997. HIV-1 cDNA integration: requirement of HMG I(Y) protein for function of preintegration complexes in vitro. Cell **88:**483–492.
26. **Feng, Y. X., S. Campbell, D. Harvin, B. Ehresmann, C. Ehresmann, and A. Rein.** 1999. The human immunodeficiency virus type 1 Gag polyprotein has nucleic acid chaperone activity: possible role in dimerization of genomic RNA and placement of tRNA on the primer binding site. J. Virol. **73:**4251–4256.
27. **Feng, Y. X., T. D. Copeland, L. E. Henderson, R. J. Gorelick, W. J. Bosche, J. G. Levin, and A. Rein.** 1996. HIV-1 nucleocapsid protein induces "maturation" of dimeric retroviral RNA in vitro. Proc. Natl. Acad. Sci. USA **93:**7577–7581.
28. **Franke, E. K., H. E. H. Yuan, K. L. Bossolt, S. P. Goff, and J. Luban.** 1994. Specificity and sequence requirements for interactions between various retroviral Gag proteins. J. Virol. **68:**5300–5305.
29. **Freed, E. O.** 1998. HIV-1 gag proteins: diverse functions in the virus life cycle. Virology **251:**1–15.
30. **Fu, W., R. J. Gorelick, and A. Rein.** 1994. Characterization of human immunodeficiency virus type 1 dimeric RNA from wild-type and protease-defective virions. J. Virol. **68:**5013–5018.
31. **Fu, W., and A. Rein.** 1993. Maturation of dimeric viral RNA of Moloney murine leukemia virus. J. Virol. **67:**5443–5449.
32. **Gallay, P., S. Swingler, J. Song, F. Bushman, and D. Trono.** 1995. HIV nuclear import is governed by the phosphotyrosine-mediated binding of matrix to the core domain of integrase. Cell **83:**569–576.
33. **Ganser, B. K., S. Li, V. Y. Klishko, J. T. Finch, and W. I. Sundquist.** 1999. Assembly and analysis of conical models for the HIV-1 core. Science **283:**80–83.
34. **Gheysen, D., E. Jacobs, F. de Foresta, C. Thiriart, M. Francotte, D. Thines, and M. DeWilde.** 1989. Assembly and release of HIV-1 precursor Pr55gag virus-like particles from recombinant baculovirus-infected insect cells. Cell **59:**103–112.
35. **Goncalves, J., Y. Korin, J. Zack, and D. Gabuzda.** 1996. Role of Vif in human immunodeficiency virus type 1 reverse transcription. J. Virol. **70:**8701–8709.
36. **Gorelick, R. J., W. Fu, T. D. Gagliardi, W. J. Bosche, A. Rein, L. E. Henderson, and L. O. Arthur.** 1999. Characterization of the block in replication of nucleocapsid protein zinc finger mutants from Moloney murine leukemia virus. J. Virol. **73:**8185–8195.
37. **Gorelick, R. J., T. D. Gagliardi, W. J. Bosche, T. A. Wiltrout, L. V. Coren, D. J. Chabot, J. D. Lifson, L. E. Henderson, and L. O. Arthur.** 1999. Strict conservation of the retroviral nucleocapsid protein zinc finger is strongly influenced by its role in viral infection processes: characterization of HIV-1 particles containing mutant nucleocapsid zinc-coordinating sequences. Virology **256:**92–104.
38. **Gross, I., H. Hohenberg, and H. G. Krausslich.** 1997. In vitro assembly properties of purified bacterially expressed capsid proteins of human immunodeficiency virus. Eur. J. Biochem. **249:**592–600.
39. **Guo, J., L. E. Henderson, J. Bess, B. Kane, and J. G. Levin.** 1997. Human immunodeficiency virus type 1 nucleocapsid protein promotes efficient strand transfer and specific viral DNA synthesis by inhibiting TAR-dependent self-priming from minus-strand strong-stop DNA. J. Virol. **71:**5178–5188.
40. **Hirt, B.** 1967. Selective extraction of polyomavirus DNA from infected mouse cell cultures. J. Mol. Biol. **26:**365–369.
41. **Housset, V., H. De Rocquigny, B. P. Roques, and J. L. Darlix.** 1993. Basic amino acids flanking the zinc finger of Moloney murine leukemia virus nucleocapsid protein NCp10 are critical for virus infectivity. J. Virol. **67:**2537–2545.
42. **Jowett, J. B., D. J. Hockley, M. V. Nermut, and I. M. Jones.** 1992. Distinct signals in human immunodeficiency virus type 1 Pr55 necessary for RNA binding and particle formation. J. Gen. Virol. **73:**3079–3086.
43. **Katz, R. A., G. Merkel, J. Kulkosky, J. Leis, and A. M. Skalka.** 1990. The avian retroviral IN protein is both necessary and sufficient for integrative recombination in vitro. Cell **63:**87–95.
44. **Kiernan, R. E., A. Ono, G. Englund, and E. O. Freed.** 1998. Role of matrix in an early postentry step in the human immunodeficiency virus type 1 life cycle. J. Virol. **72:**4116–4126.
45. **Kimpton, J., and M. Emerman.** 1992. Detection of replication-competent and pseudotyped human immunodeficiency virus with a sensitive cell line on the basis of activation of an integrated β-galactosidase gene. J. Virol. **66:**2232–2239.
46. **Kostrikis, L. G., S. Tyagi, M. M. Mhlanga, D. D. Ho, and F. R. Kramer.** 1998. Spectral genotyping of human alleles. Science **279:**1228–1229.
47. **Krausslich, H. G., and R. Welker.** 1996. Intracellular transport of retroviral capsid components. Curr. Top. Microbiol. Immunol. **214:**25–63.
48. **Lapadat-Tapolsky, M., H. De Rocquigny, D. Van Gent, B. Roques, R. Plasterk, and J. L. Darlix.** 1993. Interactions between HIV-1 nucleocapsid protein and viral DNA may have important functions in the viral life cycle. Nucleic Acids Res. **21:**831–839.
49. **Lener, D., V. Tanchou, B. P. Roques, S. F. Le Grice, and J. L. Darlix.** 1998. Involvement of HIV-I nucleocapsid protein in the recruitment of reverse transcriptase into nucleoprotein complexes formed in vitro. J. Biol. Chem. **273:**33781–33786.
50. **Lewin, S. R., M. Vesanen, L. Kostrikis, A. Hurley, M. Duran, L. Zhang, D. D. Ho, and M. Markowitz.** 1999. Use of real-time PCR and molecular beacons to detect virus replication in human immunodeficiency virus type 1-infected individuals on prolonged effective antiretroviral therapy. J. Virol. **73:**6099–6103.
51. **Lobel, L. I., J. E. Murphy, and S. P. Goff.** 1989. The palindromic LTR-LTR junction of Moloney murine leukemia virus is not an efficient substrate for proviral integration. J. Virol. **63:**2629–2637.
52. **Mak, J., M. Jiang, M. A. Wainberg, M. L. Hammarskjold, D. Rekosh, and L. Kleiman.** 1994. Role of $Pr160^{gag\text{-}pol}$ in mediating the selective incorporation of $tRNA^{Lys}$ into human immunodeficiency virus type 1 particles. J. Virol. **68:**2065–2072.

53. **Mak, J., A. Khorchid, Q. Cao, Y. Huang, I. Lowy, M. A. Parniak, V. R. Prasad, M. A. Wainberg, and L. Kleiman.** 1997. Effects of mutations in Pr160gag-pol upon tRNA(Lys3) and Pr160gag-pol incorporation into HIV-1. J. Mol. Biol. **265:**419–431.
54. **McDermott, J., L. Farrell, R. Ross, and E. Barklis.** 1996. Structural analysis of human immunodeficiency virus type 1 Gag protein interactions, using cysteine-specific reagents. J. Virol. **70:**5106–5114.
55. **Miller, M. D., C. M. Farnet, and F. D. Bushman.** 1997. Human immunodeficiency virus type 1 preintegration complexes: studies of organization and composition. J. Virol. **71:**5382–5390.
56. **Muller, H. P., and H. E. Varmus.** 1994. DNA bending creates favored sites for retroviral integration: an explanation for preferred insertion sites in nucleosomes. EMBO J. **13:**4704–4714.
57. **Myers, G., B. Korber, S. Wain-Hobson, K.-T. Jeang, L. E. Henderson, and G. N. Pavlakis.** 1994. Human retroviruses and AIDS. Los Alamos National Laboratory, Los Alamos, N. Mex.
58. **Ottmann, M., C. Gabus, and J. L. Darlix.** 1995. The central globular domain of the nucleocapsid protein of human immunodeficiency virus type 1 is critical for virion structure and infectivity. J. Virol. **69:**1778–1784.
59. **Peliska, J. A., S. Balasubramanian, D. P. Giedroc, and S. J. Benkovic.** 1994. Recombinant HIV-1 nucleocapsid protein accelerates HIV-1 reverse transcriptase catalyzed DNA strand transfer reactions and modulates RNase H activity. Biochemistry **33:**13817–13823.
60. **Poon, D. T., J. Wu, and A. Aldovini.** 1996. Charged amino acid residues of human immunodeficiency virus type 1 nucleocapsid p7 protein involved in RNA packaging and infectivity. J. Virol. **70:**6607–6616.
61. **Pruss, D., F. D. Bushman, and A. P. Wolffe.** 1994. Human immunodeficiency virus integrase directs integration to sites of severe DNA distortion within the nucleosome core. Proc. Natl. Acad. Sci. USA **91:**5913–5917.
62. **Rascle, J. B., D. Ficheux, and J. L. Darlix.** 1998. Possible roles of nucleocapsid protein of MoMuLV in the specificity of proviral DNA synthesis and in the genetic variability of the virus. J. Mol. Biol. **280:**215–225.
63. **Rein, A.** 1994. Retroviral RNA packaging: a review. Arch. Virol. Suppl. **9:**513–522.
64. **Sambrook, J., E. F. Fritsch, and T. Maniatis.** 1989. Molecular cloning: a laboratory manual, 2nd ed. Cold Spring Harbor Laboratory Press, Cold Spring Harbor, N.Y.
65. **Shank, P. R., and H. E. Varmus.** 1978. Virus-specific DNA in the cytoplasm of avian sarcoma virus-infected cells is a precursor to covalently closed circular viral DNA in the nucleus. J. Virol. **25:**104–114.
66. **Swanstrom, R., W. J. DeLorbe, J. M. Bishop, and H. E. Varmus.** 1981. Nucleotide sequence of cloned unintegrated avian sarcoma virus DNA: viral DNA contains direct and inverted repeats similar to those in transposable elements. Proc. Natl. Acad. Sci. USA **78:**124–128.
67. **Tanchou, V., C. Gabus, V. Rogemond, and J. L. Darlix.** 1995. Formation of stable and functional HIV-1 nucleoprotein complexes in vitro. J. Mol. Biol. **252:**563–571.
68. **Tsuchihashi, Z., and P. O. Brown.** 1994. DNA strand exchange and selective DNA annealing promoted by the human immunodeficiency virus type 1 nucleocapsid protein. J. Virol. **68:**5863–5870.
69. **Weiss, A., R. Wiskocil, and J. Stobo.** 1984. The role of T3 surface molecules in the activation of human T cells: a two stimulus requirement for IL-2 production reflects events occurring at a pretranslational level. J. Immunol. **133:**123–128.
70. **Wiskerchen, M., and M. A. Muesing.** 1995. Human immunodeficiency virus type 1 integrase: effects of mutations on viral ability to integrate, direct viral gene expression from unintegrated viral DNA templates, and sustain viral propagation in primary cells. J. Virol. **69:**376–386.
71. **You, J. C., and C. S. McHenry.** 1994. Human immunodeficiency virus nucleocapsid protein accelerates strand transfer of the terminally redundant sequences involved in reverse transcription. J. Biol. Chem. **269:**31491–31495.